JMEPEG (2003) 12:48-55

Metal/Quenchant Interfacial Heat Flux Transients During Quenching in Conventional Quench Media and Vegetable Oils

K. Narayan Prabhu and Amlan Prasad

(Submitted 9 July 2002)

The determination of quench severity and the quantification of the boundary conditions at the metal/quenchant interface would be of considerable utility to the heat treating community. In the present work, an attempt has been made to determine the quench severity of various quench media, including three vegetable oils, by the Grossmann Hardenability Factor method and by estimation of heat flux transients by inverse modeling of heat conduction in 304 stainless steel quench probes. The heat flux transient technique was found to be more accurate than the Grossmann technique in assessing the severity of quenching. This finding was supported by the hardness data and microstructure obtained with the quenched steel specimens. New heat flux parameters are proposed to assess the severity of quenching. The boundary heat flux transients during end quenching of AISI 1040 steel specimens were also estimated. The estimated heat flux transients could be used for modeling of heat transfer during quenching. An attempt has also been made in the present work to assess the feasibility of three vegetable oils, namely coconut, sunflower, and groundnut oils, as quenching media. Further investigation is required in this direction to explore the suitability of these oils for industrial heat treating applications. This application would have immense environmental and economical benefits.

Keywords heat flux, inverse modeling, metal/quenchant interface, quench severity, vegetable oils

1. Introduction

Quenching refers to rapid cooling of metal parts from the solution-treating temperature, typically in the range of 845-870 °C for steel alloys. Quenching is performed to prevent ferrite or pearlite formation and allow bainite or martensite to be formed. Quenching of steel in liquid medium consists of three distinct stages of cooling: vapor phase, nucleate boiling, and convective stage.[1,2] In the first stage, a vapor blanket is formed immediately upon quenching. This blanket has an insulating effect and heat transfer in this stage is slow, since it is mostly through radiation. Fletcher and Griffiths carried out a photographic study of the appearance of the vapor-liquid mixture adjacent to a steel plate quenched in sodium polyacrylate quenchants.[3] The duration of the vapor blanket stage increased with increase in polymer concentration. As the temperature drops, the vapor blanket becomes unstable and collapses, initiating the nucleate boiling stage. Heat removal is the fastest in this stage, due to the heat of vaporization, and continues until the surface temperature drops below the boiling point of the quenching medium. Further cooling takes place mostly through convection and some conduction. The rate of heat transfer from the workpiece to the quench medium is thus the most critical information relating to the hardening process.

K. Narayan Prabhu and **Amlan Prasad,** Department of Metallurgical & Materials Engineering, National Institute of Technology Karnataka, Surathkal, P.O. Srinivasnagar 575 025 Karnataka State, India. Contact e-mail: prabhukn_2002@yahoo.co.in.

Achieving the required hardness, strength, or toughness, and minimizing the possibility of occurrence of quench cracks due to the evolution of residual stresses are the key indicators of a successful hardening process.[4] Expensive, high value-added parts become scrap if insufficient attention is paid to proper quenching. Selection of a quenchant is primarily governed by the processing specifications, the required physical properties, and the required microstructure. Hence, the determination of quench severity and the quantification of the boundary conditions at the metal/quenchant interface would be of considerable utility to the heat treating community. Simulation based quench process design would enable the heat treater to judiciously select the quench medium for a specific application.[5]

For successful simulation of heat transfer during the quenching process, a reliable database on the heat flux transients at the metal/quenchant interface is essential to accurately predict the temperature distribution and the cooling rates inside the part being quenched. The temperature distribution could further be used to carry out a coupled heat transfer/thermal stress analysis to predict the evolution of quench cracks and the distortion of the part. The right method for getting the realistic metal/quenchant interfacial heat transfer properties is inverse modeling and this method allows the determination of boundary conditions by the coupling of numerical methods with simple temperature measurements inside the quench probe.[6]

Quench probes made up of stainless steel and Inconel 600 have been used by several researchers to determine the quench severity of the quenchant.[7-9] Although this method could be used to characterize several quench media, it does not give any information on the heat transfer characteristics of different grades of steel specimens subjected to quenching in various quench media. Lumped heat capacity method is only an approximate technique to determine the heat transfer coefficients, as this method assumes a constant workpiece temperature. Kobasko et al. experimentally determined the first and second critical heat flux densities to characterize the quenching process.[10] A two-dimensional inverse method combined with the lumped heat capacity method was adopted by Narazaki et al. to estimate the heat transfer coefficients.[11]

Most of the work carried out on heat transfer during quenching has been devoted to the estimation of cooling power of the quench media and not much attention is given to the heat transfer-structure-property correlation during quenching of steel specimens. In this investigation, an attempt has been made to determine the heat flux transients during quenching of a medium carbon steel probe and correlate the results to its microstructure and hardness. A method to express quench severity in terms of the heat flow at the specimen/quenchant interface is also proposed. The effect of calculated quench severity of water, brine, and mineral and vegetable oils on microstructure and hardness of medium carbon steel are investigated. Quenching with vegetable oils is examined, as these oils are environment friendly and solve the problem of oil disposal.

2. Experiment

The experimental setup consisted of a vertical tubular electric resistance furnace open at both ends. A beaker containing 2000 mL of quenchant was placed directly underneath the furnace so that the heated probe could be transferred quickly to the quenching medium. Water, 10% brine, and a mineral oil (Indian Oil Corp., Mumbai, Maharashtra, India) were selected as the quench media. Apart from these conventional quenchants, three locally available vegetable oils, namely coconut, sunflower, and groundnut oils, were used. Quench probes for end and lateral quenching were prepared from AISI 304 (Mukand Ltd., Mumbai, Maharashtra, India) and 1040 (Rashtriya Ispat Nigam Ltd., Visakhapatnam, Andhra Pradesh, India) steels and used to assess quench severity and assessment of metal/quenchant interfacial heat transfer. All the probes were instrumented with K-type thermocouples of 0.45 mm diameter. The dimensions of the probes and the location of the thermocouples are given in Fig. 1 and 2, respectively. All of the thermocouples were connected by means of compensating cables to the datalogger interfaced with the computer. The probe was heated to 850 °C in an electric resistance furnace and held vertically inside the furnace using a nichrome wire for 5 min and was quickly transferred to a beaker containing 2000 mL of the quenchant.

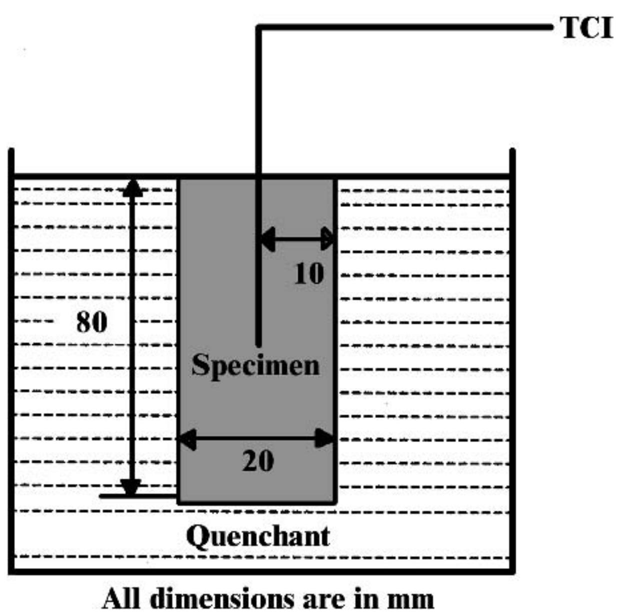

Fig. 1 Schematic sketch of the lateral quenching setup

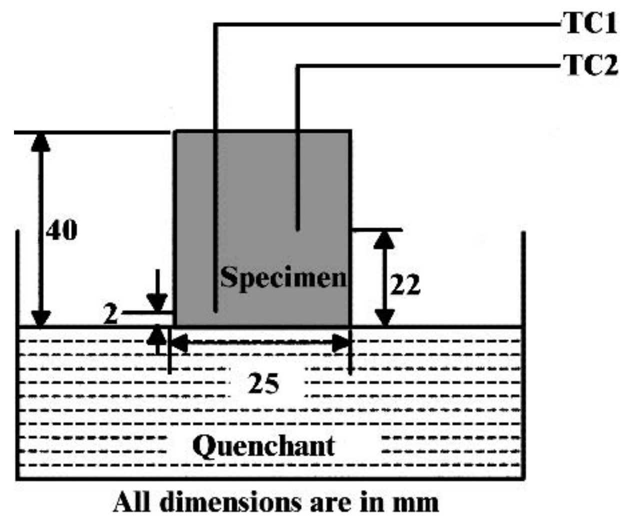

Fig. 2 Schematic sketch of the end quenching setup

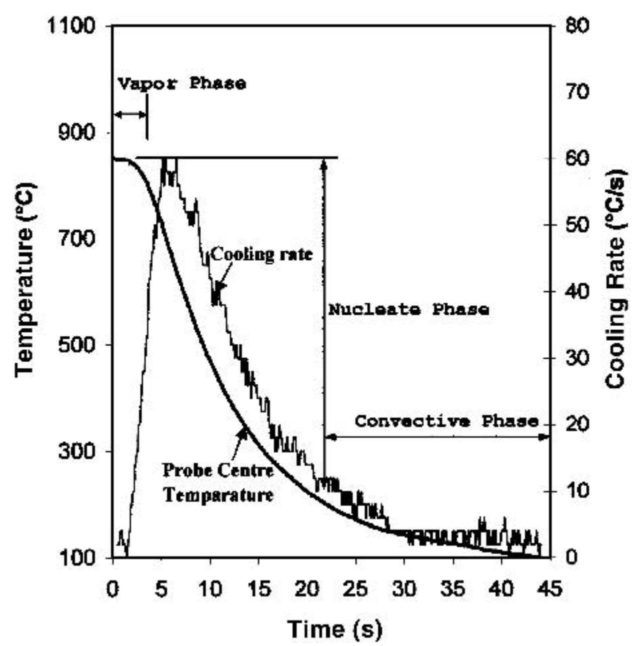

Fig. 3 Thermal history at the geometric center of the stainless steel probe and the estimated cooling rates during lateral quenching in 10% brine

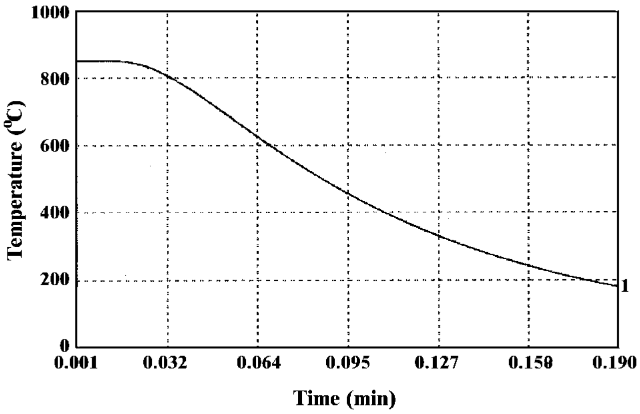

Fig. 4 Simulated cooling curve for Ø 20 mm × 80 mm stainless steel probe, $H = 5$ in^{-1} and $h = 6811$ W/m^2 · K

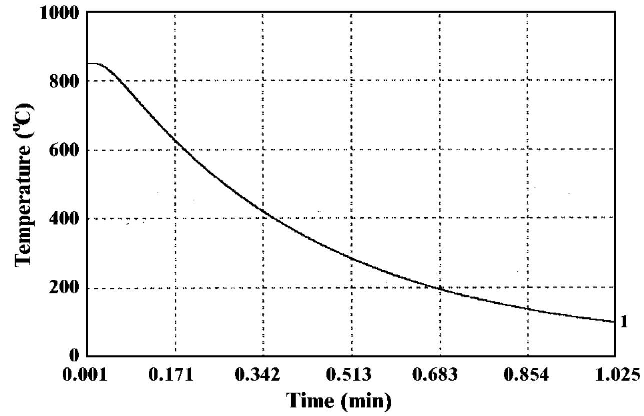

Fig. 5 Simulated cooling curve for Ø 20 mm × 80 mm stainless steel probe, $H = 0.5$ in^{-1} and $h = 681$ W/m^2 · K

Table 1 Measured Cooling Rate Parameters

Quench Media → Cooling Rate Parameter ↓	10% Brine	Water	Sunflower Oil	Coconut Oil	Groundnut Oil	Mineral Oil
Maximum cooling rate (°C/s)	70	50	50	45	40	40
Temperature at maximum cooling rate (°C/s)	690	682	659	620	666	523
Cooling rate at 300 °C (°C/s)	30	20	20	10	10	10
Time to reach 600 °C (s)	7.3	8.9	10.7	13.4	11.1	23.6
Time to reach 400 °C (s)	11.9	14.4	18.6	20.8	20.6	32.8
Time to reach 200 °C (s)	22.0	25.1	64.9	50.8	66.4	49.2

Table 2 Viscosity, mPa · s of Various Quenching Oils at 27 °C

Mineral Oil	Groundnut Oil	Sunflower Oil	Coconut Oil
57.24	48.15	43.02	36.53

The following sets of experiments were carried out:

1) Lateral quenching of AISI 304 stainless steel probe to assess the quench severity using the Grossmann Hardenability Factor technique;
2) End quenching of AISI 304 steel specimens to assess the severity of quenching by estimating the surface heat flux transients;
3) Immersion quenching of AISI 1040 steel 25 mm diameter disk specimens to assess the effect of quench severity, as measured by experiments 1 and 2 on hardness and microstructure;
4) End quenching of medium carbon AISI 1040 steel probes in various quenchants to assess the metal/quenchant interfacial heat flux transient boundary condition; and
5) Measurement of hardness in the quenched AISI 1040 steel specimens at various locations from the quenched end.

3. Results and Discussion

Figure 3 shows the typical thermal history and cooling rates at the center of the AISI 304 stainless steel probe subjected to lateral quenching in 10% brine. Various stages of quenching are marked in the figure.

Based on the cooling curves, the following thermal analysis parameters were determined:

- peak cooling rate,
- temperature at which the maximum cooling rate occurs,
- cooling rate at 300 °C, and
- cooling time to 600, 400, and 200 °C.

These data are given in Table 1. A higher peak cooling rate of 70 °C/s was obtained with the brine solution. However, the groundnut and mineral oils resulted in a lowest peak cooling rate of about 40 °C/s. The cooling rate of the quench probe was found to be strongly dependent on viscosity of the quench media. Oils with higher viscosity resulted in decreased cooling rates. The viscosities of all of the oil quenchants measured at 27 °C are given in Table 2. The viscosities of water and brine solution at 27 °C are 1 mPa · s and 2 mPa · s, respectively.[12]

4. Determination of Quench Severity by Grossmann Technique

The quench process was simulated using the AFS 3D software package (Finite Solutions Inc., Cincinnati, OH). Analytical cooling curves were obtained from the simulation for a stainless steel probe of diameter 20 mm and height 80 mm with eight different quench severity values (H) imposed on the

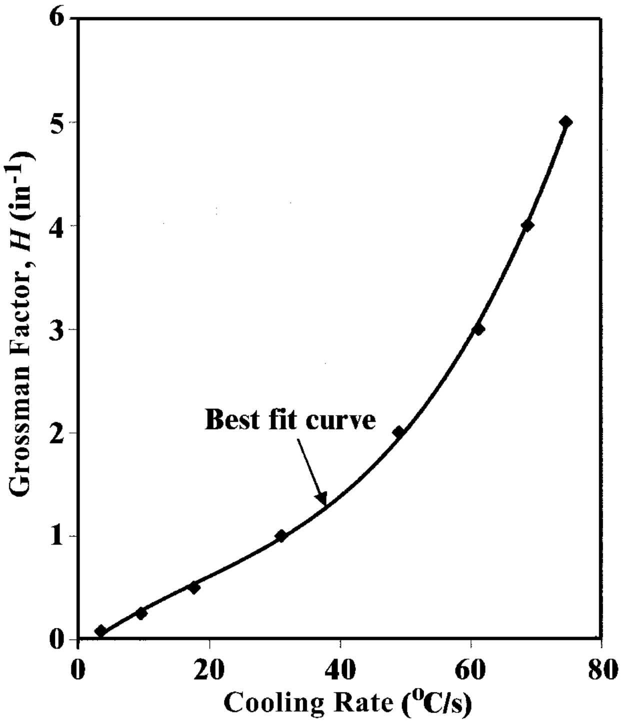

Fig. 6 Grossmann Hardenability Factor vs cooling rate

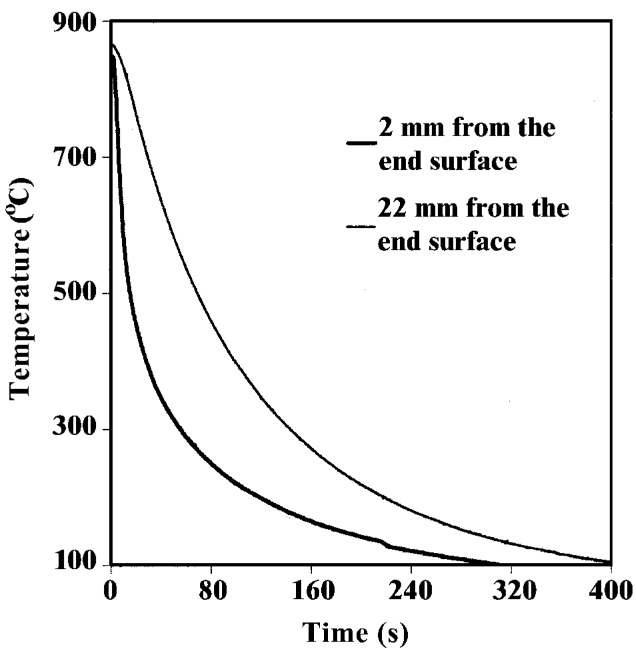

Fig. 7 Temperature-time curve obtained during end quenching of stainless steel probe in 10% brine

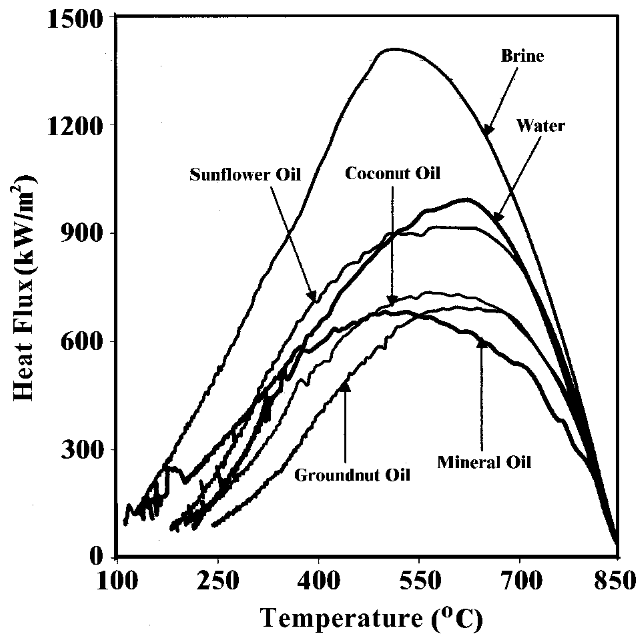

Fig. 8 Variation of heat flux with probe surface temperature during end quenching of stainless steel probe in various quench media

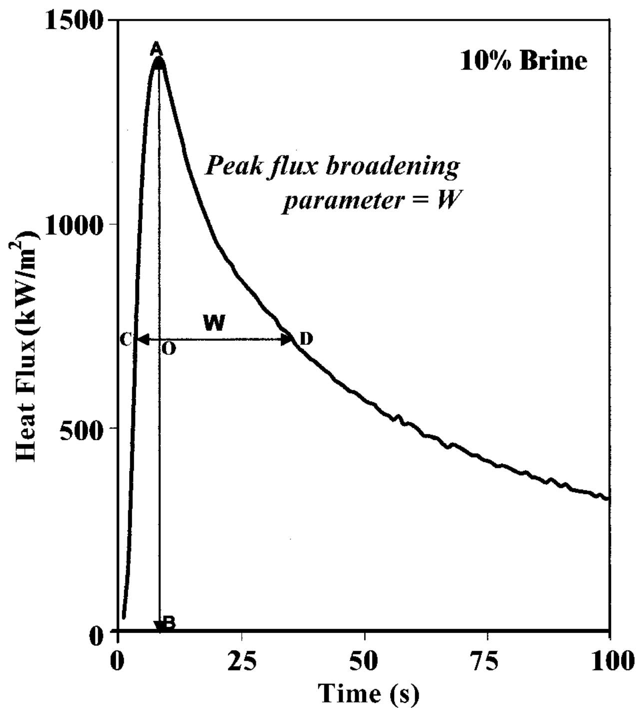

Fig. 9 Measurement of peak flux broadening parameter

metal/quenching interface. The corresponding heat transfer coefficients (h) were calculated using the relation,

$$H = h/2k \quad \text{(Eq 1)}$$

where "k" is the thermal conductivity of the probe material and was taken as 17.3 W/m K.

A virtual thermocouple was inserted at the center of the probe in the simulation to obtain the thermal history. Figures 4 and 5 show the typical analytical cooling curves computed for quench severity values of 5 in^{-1} and 0.5 in^{-1}, respectively. The cooling rate was calculated using the time required to cool from 730-260 °C at the center. A plot of cooling rate versus Grossmann Hardenability Factor, H is shown in Fig. 6. The cooling

Table 3 Comparison of Grossmann and Heat Flux Quench Severity Data

Quenching Medium	Hardness for AISI 1040 Button Specimen, R_C	Grossman Hardenability Factor, H, in^{-1}	Peak Heat Flux, kW/m^2	Total Heat Flow for 250 s, MJ/m^2	Peak Flux Broadening Parameter, s
Brine	63	0.99	1407	90	32
Water	62	0.87	987	84	53
Sunflower Oil	53	0.45	914	78	59
Coconut Oil	51	0.48	733	73	63
Groundnut Oil	47	0.40	692	67	68
Mineral Oil	46	0.46	680	72	83

rate increased as H increased. The variation of the cooling rate with H could be described by a polynomial equation of the type

$$H\ (in^{-1}) = 1 \times 10^{-5} \times (°C/s)^3 - 0.0008 \times (°C/s)^2 + 0.0453 \times (°C/s) - 0.0951 \qquad \text{(Eq 2)}$$

Equation 2 enables the estimation of quench severity of any quenching medium from knowledge of experimentally determined cooling rates. The severity of quench media used in the present investigation estimated from the above equation could be arranged in the following descending order:

Brine (H = 0.99 in^{-1})
> Water (H = 0.87 in^{-1})
> Coconut Oil (H = 0.48 in^{-1})
> Mineral Oil (H = 0.46 in^{-1})
> Sunflower Oil (H = 0.45 in^{-1})
> Groundnut Oil (H = 0.40 in^{-1})

5. Determination of Quench Severity by Inverse Analysis

The inverse modeling of heat conduction enables the determination of boundary heat flux transients and the specimen surface temperature. This method overcomes the limitation of the Grossmann technique in handling time varying heat transfer coefficients.

Figure 7 shows the thermal history measured at two locations (one near and another far from the metal/quenchant interface) during end quenching of the AISI 304 stainless steel probe in 10% brine. The measured temperature history was used as an input to an inverse heat conduction model to estimate the heat flux transients at the metal/quenchant interface. The mathematical details of the inverse analysis are given in Ref. 13 and 14. The inverse analysis also yielded the temperature of the probe surface in contact with the quench medium.

Figure 8 shows the estimated heat flux versus surface temperature profile during end quenching of the stainless steel probe in various quench media used in the present investigation. The heat flux transients showed a peak during nucleate boiling stage for all the quenchants. The occurrence of a peak in the heat flux curve can be associated with the peak thermal gradient existing inside the quenched specimen. The water and brine quenchants showed a sharp peak compared with that obtained with oil quenchants. The occurrence of a peak was followed by a drastic decrease in the heat flux transients at the specimen/quenchant interface, indicating negligible thermal gradients inside the specimen at the later stages of cooling. A maximum heat flux of 1407 kW/m^2 was obtained with 10% brine solution. The mineral oil yielded the lowest peak heat flux value of 680 kW/m^2. The area under the heat flux transient curve gives the total heat removed from the specimen in a given interval of time. In the present work, total heat flow was computed for a time interval of 250 s. The broadening of the peak of the heat flux transients in the case of oil quenchants is probably due to the effect of viscosity in maintaining a uniform thermal gradient in the specimen for a longer duration of time. The thinning of oil at higher temperatures offsets the effect of increase in temperature and thus maintains peak heat transfer rates for a longer time. A peak flux broadening parameter proposed to quantify the broadening of the heat flux transient curve at the peak and was evaluated by measuring the width W, in seconds, at a heat flux transient equal to half the peak heat flux (Fig. 9). The broadening parameter was found to be minimum for brine (32 s) and was maximum for the mineral oil quenchants (83 s). The peak heat flux (W/m^2), the integral heat flow (J/m^2), and peak flux broadening parameters thus could be used as a measure of quench severity of the various quench media.

Based on the heat flux parameters, the severity of quench media used in the present investigation could be arranged in the following descending order.

Brine > Water > Sunflower Oil > Coconut Oil
> Groundnut Oil > Mineral Oil

Table 3 gives a comparison of the quench severity measured by various techniques and its influence on hardness obtained for AISI 1040 disk steel specimens. It is interesting to note that the mineral oil which yielded the lowest severity of quenching resulted in quenched specimens having lower values of hardness compared with that obtained with other quench media. In the case of the Grossmann technique, the severity of quenching of mineral oil was found greater than sunflower and groundnut oils, although specimens quenched in mineral oil showed lower hardness. This could be attributed to the Grossmann Hardenability Factor technique's limitation of determination of quench severity (taking into account the transient nature of the specimen/quenchant interfacial heat transfer). Further, the simulation of heat transfer was based on a single value of boundary heat transfer coefficient, although in reality "h" is a strong function of the specimen surface's temperature in contact with the quench medium. Hence, the heat flux transient technique is superior to the Grossmann technique for assessing the severity of quenching of quench media.

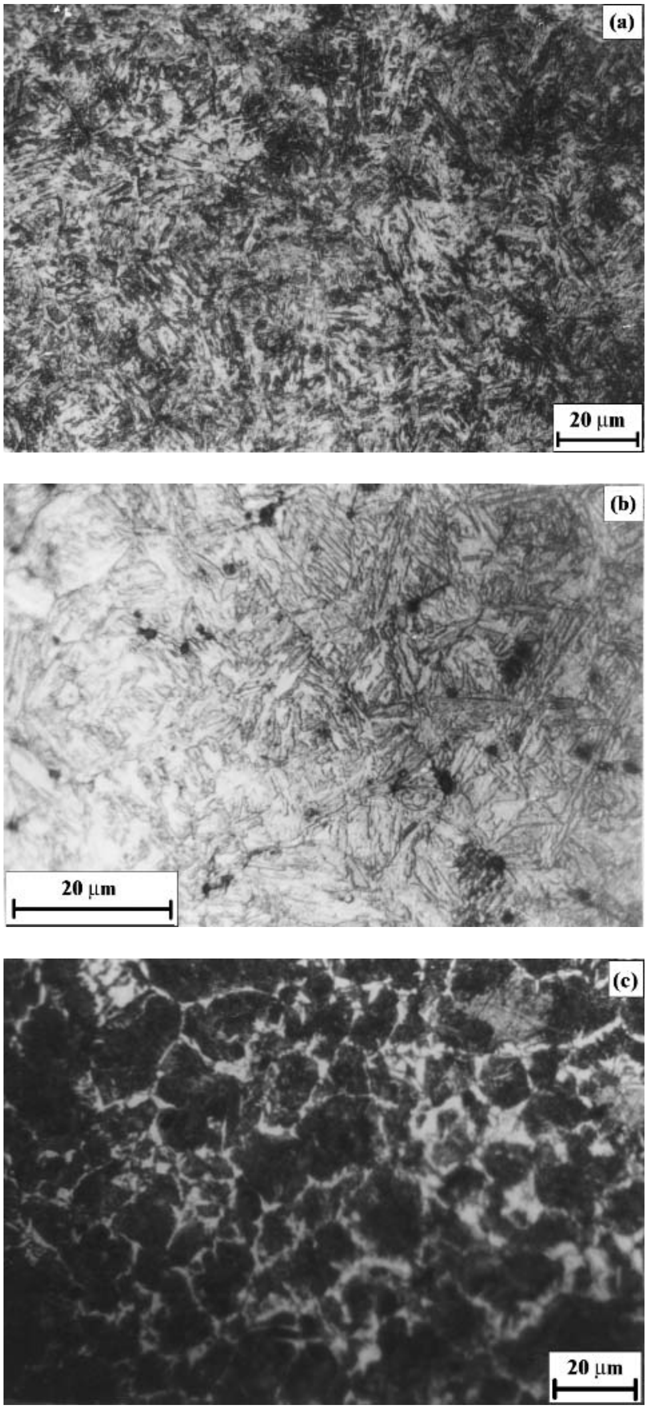

Fig. 10 Microstructure of AISI 1040 steel disk specimens quenched in conventional quench media: **(a)** 10% brine, **(b)** water, **(c)** mineral oil

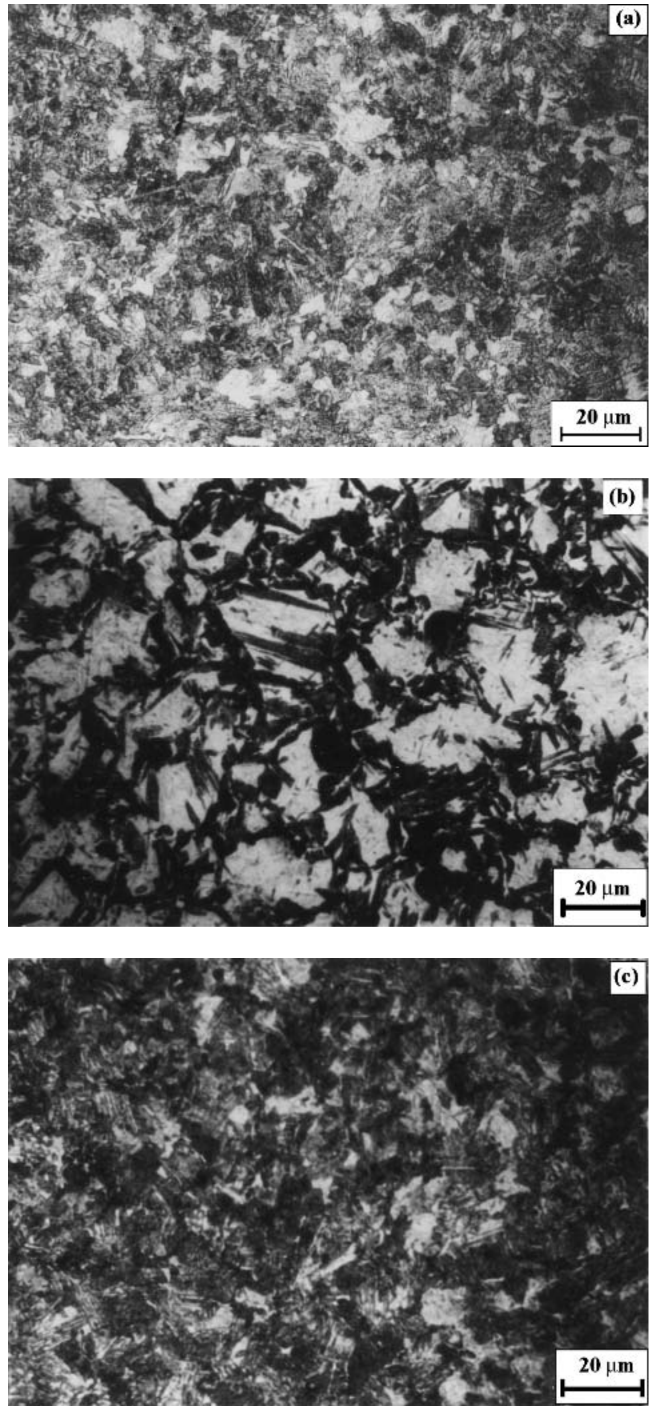

Fig. 11 Microstructure of AISI 1040 steel disk specimens quenched in three vegetable oils: **(a)** sunflower oil, **(b)** coconut oil, **(c)** groundnut oil

Figure 10(a-c) shows the photomicrographs of the AISI 1040 steel disk specimens quenched in 10% brine, water, and mineral oil. The water and brine quenched disk specimens clearly showed martensitic structure (Fig. 10a,b). In the case of mineral oil, the microstructure consisted mainly of ferrite and pearlite (Fig. 10c). The photomicrographs of specimens quenched in vegetable oils showed a mixed microstructure consisting of martensite and bainite (Fig. 11a-c). The extent of formation of martensite is larger for specimens quenched in sunflower and coconut oils. This was in agreement with the measured hardness of these specimens (see Table 3). The results clearly showed that the vegetable oils had higher quenching power compared with the mineral oil. It was also experimentally found that the flash point of vegetable oils was in the

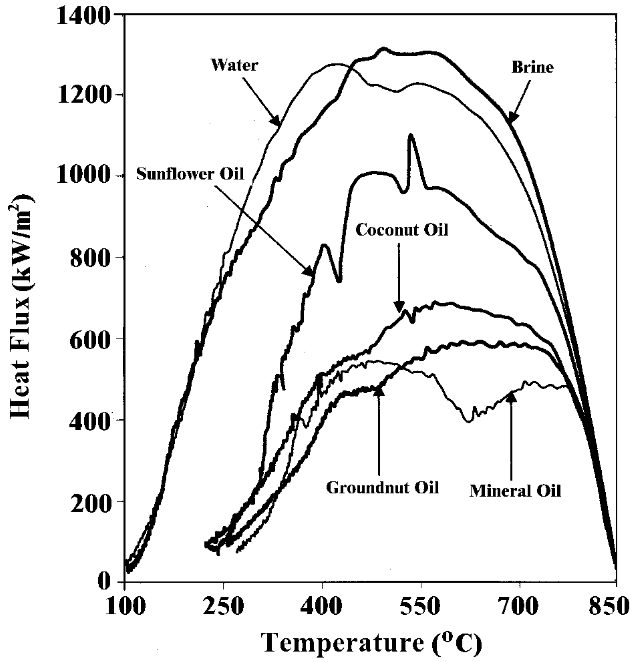

Fig. 12 Variation of heat flux with probe surface temperature during end quenching of AISI 1040 steel probe in various quench media

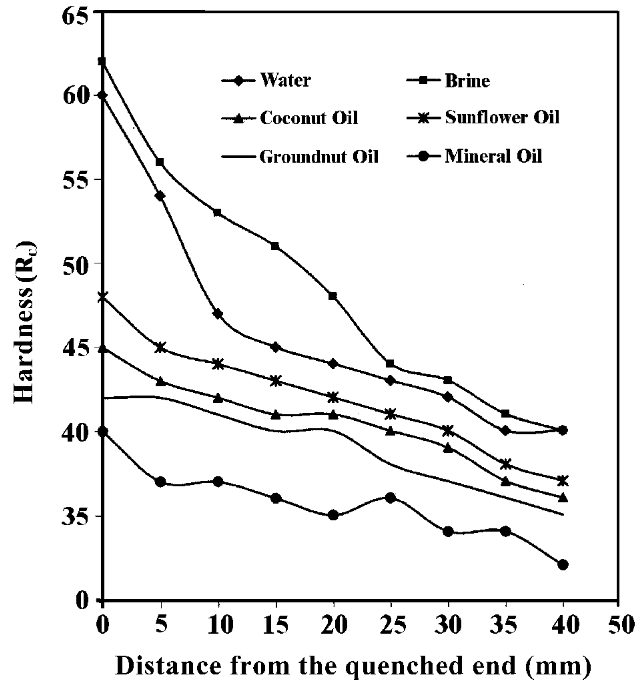

Fig. 13 Variation of hardness from the probe surface for the end quenched AISI 1040 steel probe

range of 325-350 °C compared with 250 °C measured for the mineral oil.

Brine quenched specimens showed higher hardness than water quenched samples, although the viscosity of brine is more than twice that of water. This is due to the existence of a stable vapor phase film in the case of water quenching. During quenching with brine, it is likely that a localized increase in the concentration of the sodium chloride would occur near the specimen due to the evaporation of water. This could result in the destabilization of the insulating vapor blanket, increasing the rate of heat transfer from the specimen to the quench medium.

6. Heat Flux Transients During End Quenching of AISI 1040 Grade Steel

The actual boundary heat flux transients during quenching of a particular grade of steel would be extremely useful to a modeler of heat treatment operations to compute the temperature distribution inside the specimen being quenched. In the present work, the thermal history inside a medium carbon AISI 1040 grade steel probe during end quenching was used for estimating probe surface/quenchant interfacial heat flux transients using inverse analysis. Figure 12 shows the variation of estimated heat flux transients with probe surface temperature. The heat transfer was a maximum for brine and water. Lower heat transfer rates were obtained with mineral oil. Figure 13 shows the hardness plotted as a function of distance from the quenched end. The hardness values agreed well with the heat flux transients at the metal/quenchant interface estimated for various quench media.

7. Conclusions

Based on the results and discussion, the following conclusions were drawn:

1) The effect of cooling rate (°C/s) on the Grossmann Hardenability Factor (in^{-1}) during quenching of a stainless steel probe was quantified by an equation,

$$H\ (in^{-1}) = 1 \times 10^{-5} \times (°C/s)^3 - 0.0008 \times (°C/s)^2 + 0.0453 \times (°C/s) - 0.0951$$

This equation could be used to compare the severity of quenching of unknown quench media from knowledge of the specimen cooling rates. Accordingly, the severity of quenching for the quenchants used in the present work are arranged in the following descending order

Brine > Water > Coconut Oil > Mineral Oil
> Sunflower Oil > Groundnut Oil

2) Although mineral oil had a higher Grossmann Hardenability Factor than sunflower and groundnut oils, the hardness data measured on disk specimens of medium carbon steel quenched in these oils indicated slightly opposing results. This was attributed to the assumption of a constant heat transfer coefficient in the simulation of heat transfer for estimating the effect of cooling rate on the Grossmann Hardenability Factor.
3) The limitation of the Grossmann technique in handling the transient heat transfer coefficients was overcome by estimating the boundary heat flux transients during end quenching of stainless steel probes using an inverse analysis. The

peak heat flux, integral heat flow, and peak flux broadening parameters estimated during quenching could be used as measures of quench severity. The peak flux broadening parameter was influenced by the viscosity of the quench medium used in the present investigation.

4) Based on the values of various heat flux parameters, the severity of quenching of the various quench media can be arranged in the following order.

   Brine > Water > Sunflower Oil > Coconut Oil
   > Groundnut Oil > Mineral Oil

   These results were in complete agreement with the metallurgical microstructure and the hardness data obtained with the steel specimens. A martensitic structure was obtained for water and brine quenched disk steel specimens. Specimens quenched in vegetable oils showed a mixed microstructure consisting mainly of martensite and bainite. The microstructure of specimens quenched in mineral oil consisted significantly of ferrite and pearlite.

5) Inverse modeling of heat transfer was extended to the end quenching of AISI 1040 steel probes to estimate the boundary heat flux transients. Heat flux transients for various quenchants indicated the occurrence of peak heat flux in the nucleate boiling regimen. The brine solution yielded the maximum peak heat flux of 1310 kW/m^2. Lowest peak heat flux value of 543 kW/m^2 was obtained in the case of mineral oil.

6) Analysis of heat transfer, microstructure, and hardness data showed that the quenching power of the three vegetable oils considered in this work is better than that of mineral oil.

References

1. J.R. Easterday: "Heat Treating" in *Metals Handbook*, Vol. 4, 9th ed., ASM International, Materials Park, OH, 1981, pp. 31-69.
2. G.E. Totten, C.E. Bates, and N.A. Clinton: *Handbook of Quenching and Quenching Technology*, ASM International, Materials Park, OH, 1993, pp. 1-160.
3. A.J. Fletcher and W.D. Griffiths: "Quenching of Steel Plates in Sodium Polyacrylate Solutions," *Mater. Sci. Technol.*, 1993, *9*, pp. 176-82.
4. G.E. Totten, Y. Sun, G.M. Webster, L.M. Jarvis, and C.E. Bates: "Quenchant Selection" in *Proc. 18th Conference of Heat Treating Symposium Including the Lui Dai Memorial Symposium,* ASM International, Materials Park, OH, 1998, pp. 183-89.
5. C. Tszeng and P. Nash: "Modelling Heat Treating Processes," *Indust. Heating*, 2001, *68*, pp. 12-14.
6. B. Liscic: "State of the Art in Quenching" in *Proc. 3rd Seminar of the International Federation for Heat Treatment and Surface Engineering,* The Institute of Materials, London, UK, 1993, pp. 1-32.
7. J. Bodin and S. Segerberg: "Measurement and Evaluation of the Quenching Power of Quenching Media for Hardening" in *Proc. 3rd Seminar of the International Federation for Heat Treatment and Surface Engineering*, The Institute of Materials, London, UK, pp. 33-54.
8. C.E. Bates, G.E. Totten, and K.B. Orszak: "Quench Severity Effects on the Properties of Selected Steel Alloys" in *Proc. 3rd Seminar of the International Federation for Heat Treatment and Surface Engineering*, The Institute of Materials, London, UK, pp. 55-69.
9. C.E. Bates and G.E. Totten: "Estimating Quench Severity With Cooling Curves I," *Indust. Heating*, 1992, *59*, pp. 24-26.
10. N.I. Kobasko, A.A. Moskalenko, G.E. Totten, and G.M. Webster: "Experimental Determination of the First and Second Critical Heat Flux Densities and Quench Process Characterization," *J. Mater. Eng. Performance*, 1997, *6*, pp. 93-101.
11. M. Narazaki, M. Kogawara, A. Shirayori, and S. Fuchizawa: "Accuracy of Evaluation Methods for Heat Transfer Coefficients in Quenching" in *Proc. 18th Conference of Heat Treating Symposium Including the Lui Dai Memorial Symposium*, ASM International, Materials Park, OH, 1998, pp. 509-17.
12. G.H. Geiger and D.R. Poirier: *Transport Phenomena in Materials Processing,* Minerals, Metals & Materials Society, Warrendale, PA, 1994, p. 17.
13. T.S. Prasanna Kumar and K. Narayan Prabhu: "Heat Flux Transients at the Casting/Chill Interface During Solidification of Aluminium Base Alloys," *Metall. Trans. B*, 1991, *22B*, pp. 717-27.
14. J.V. Beck: "Nonlinear Estimation Applied to the Nonlinear Heat Conduction Problem," *J. Heat Transfer*, 1970, *13*, pp. 713-16.